EPJ Web of Conferences **37**, 03005 (2012)
DOI: 10.1051/epjconf/20123703005

Combined analysis of $\gamma N \to \eta' N$, $\pi N \to \eta' N$ and $NN \to NN\eta'$ reactions

F. Huang[1,a], H. Haberzettl[2], and K. Nakayama[1,3]

[1] Department of Physics and Astronomy, The University of Georgia, Athens, GA 30602, USA
[2] Institute for Nuclear Studies and Department of Physics, The George Washington University, Washington, DC 20052, USA
[3] Institut für Kernphysik (Theorie) and Jülich Center for Hadron Physics, Forschungszentrum-Jülich, 52425 Jülich, Germany

Abstract. A combined analysis of the free and quasi-free $\gamma N \to \eta' N$, $NN \to NN\eta'$, and $\pi N \to \eta' N$ reactions has been performed within an effective Lagrangian approach. It is found that a set of above-threshold resonances $\{S_{11}, P_{11}, P_{13}\}$, with fitted mass values of about M_R = 1925, 2130, and 2050 MeV, respectively, and the four-star sub-threshold $P_{13}(1720)$ resonance reproduce best all existing data for the η' production processes in the resonance-energy region up to $\sqrt{s}$ = 2.35 GeV.

1 Introduction

The η' meson is much heavier than the pion, and thus η' meson-production processes near threshold are well suited for investigating high-mass resonances in low partial-wave states. Moreover, reaction processes such as η' photoproduction provide opportunities to study the problem of the so-called "missing resonances", as those resonances may couple weakly to pions but strongly to other channels.

In this work, we consider spin-1/2 and 3/2 resonances in an effective Lagrangian approach to analyze the new photoproduction data [1–3], the $\pi N \to \eta' N$ total cross section data, and the cross section and NN and $N\eta'$ invariant mass distribution data for $NN \to NN\eta'$. In the study of $NN \to NN\eta'$ reaction, we use the Distorted Wave Born Approximation (DWBA) where both the initial- and final-state NN interaction are taken into account explicitly. We found that a minimum set of three above-threshold resonances $\{S_{11}, P_{11}, P_{13}\}$, with the masses of about M_R = 1925, 2130 and 2050 MeV, respectively, and the well-established below-threshold resonance $P_{13}(1720)$ is needed to describe all the existing data for the η' production processes in the resonance-energy region up to $\sqrt{s}$ = 2.35 GeV. These three above-threshold resonances may be tentatively identified with the corresponding $S_{11}(1895)$**, $P_{11}(2100)$*, and $P_{13}(2040)$* resonances listed in PDG [4].

2 Results

The results presented here are from our recent work [5] on a combined analysis of η' production processes for the reactions $\gamma N \to \eta' N$, $\pi N \to \eta' N$ and $NN \to NN\eta'$. The reader is referred to our original paper [5] for details.

As discussed in Ref. [5], there is discrepancy between the CLAS [1] and CBELSA/TAPS [2] data for $\gamma p \to \eta' p$. Thus we consider them separately in our combined analysis of η' production processes. Figure 1 shows our resulting independent fit curves for the CLAS and CBELSA/TAPS data. We see that both data sets are reproduced very well. The fitted model parameters are listed in

[a] e-mail: huang@physast.uga.edu

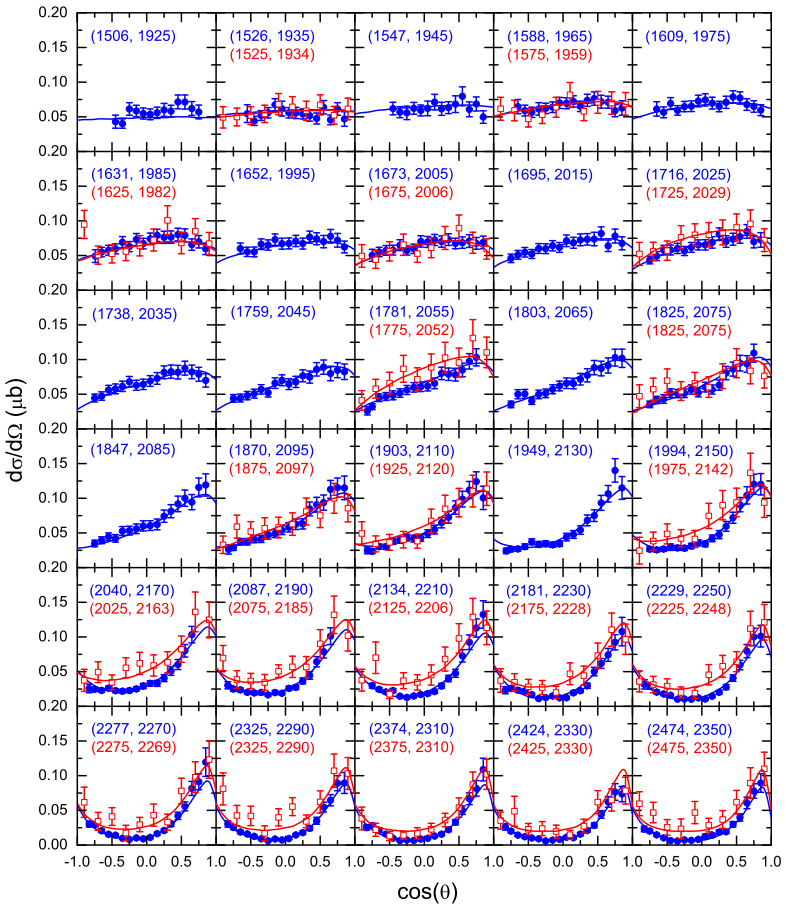

Fig. 1. (Color online) Differential cross sections for $\gamma p \to \eta' p$. The blue and red curves are our results fitted to CLAS data [1] (filled circles) and CBELSA/TAPS data [2] (empty squares), respectively.

Table I of Ref. [5]. All the resonance masses and widths from the fit to CLAS data are very close to those from the fit to CBELSA/TAPS data, except for the width of $P_{13}(2050)$ resonance, for which the CBELSA/TAPS data yield a much narrower width, however, with a very large uncertainty.

Figure 2 shows our results for quasi-free $\gamma p \to \eta' p$. The dashed and short-dashed curves are our model predictions. They differ from the quasi-free data. The possible reason is either our prescription is inadequate for accounting for the Fermi motion or the quasi-free data contain additional nuclear effects which cannot be adequately described by the simple folding procedure. The solid curves in Fig. 2 are our fit results of the $\gamma p \to \eta' p$ quasi-free data. We see the data are described well. The fitted resonance parameters and the individual resonance contributions are shown and discussed in Ref. [5].

Figure 3 shows our results for quasi-free $\gamma n \to \eta' n$. We see that overall, the data are reproduced reasonably well.

Figure 4 shows our results for the η' angular distribution in $pp \to pp\eta'$ at the excess energies of $Q = 46.6$ and 143.8 MeV, and Fig. 5 shows the $\pi N \to \eta' N$ total cross sections. These results are obtained in conjunction with the CLAS photoproduction data. Again, all the data are reproduced quite well. See Ref. [5] for the discussion of contributions from individual currents/partial-waves.

We emphasize that in a combined analysis of η' photon- and hadron-induced reactions, $\{P_{13}(1720), S_{11}(1925), P_{13}(2050), P_{11}(2130)\}$ is the minimum set of resonances to describe well all the existing data in the energy region considered in this work.

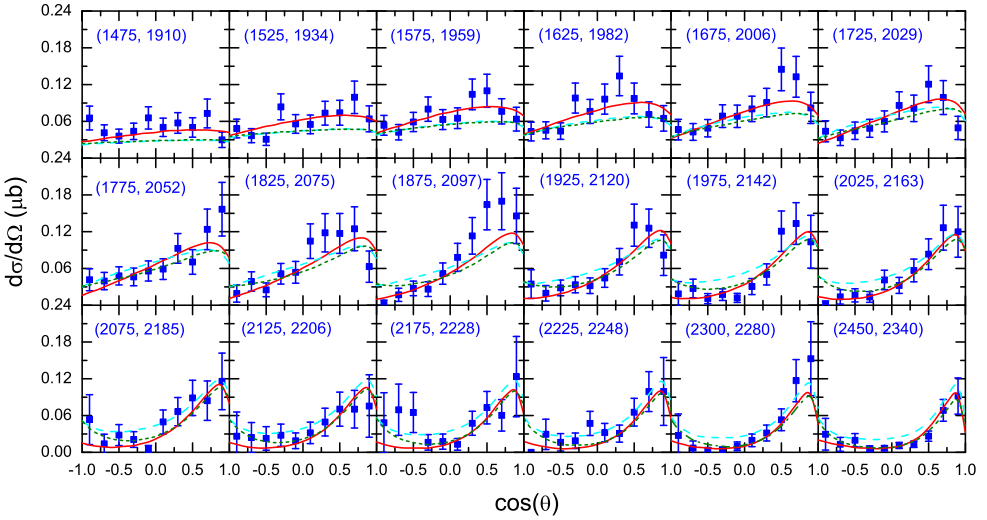

Fig. 2. (Color online) Differential cross sections for quasi-free $\gamma p \to \eta' p$. The solid curves are our results fitted to the CBELSA/TAPS quasi-free data [3] (solid squares). The (cyan) dashed and the (olive) short-dashed curves are obtained by respectively folding our free cross section results fitted to CBELSA/TAPS and CLAS data (Fig. 1).

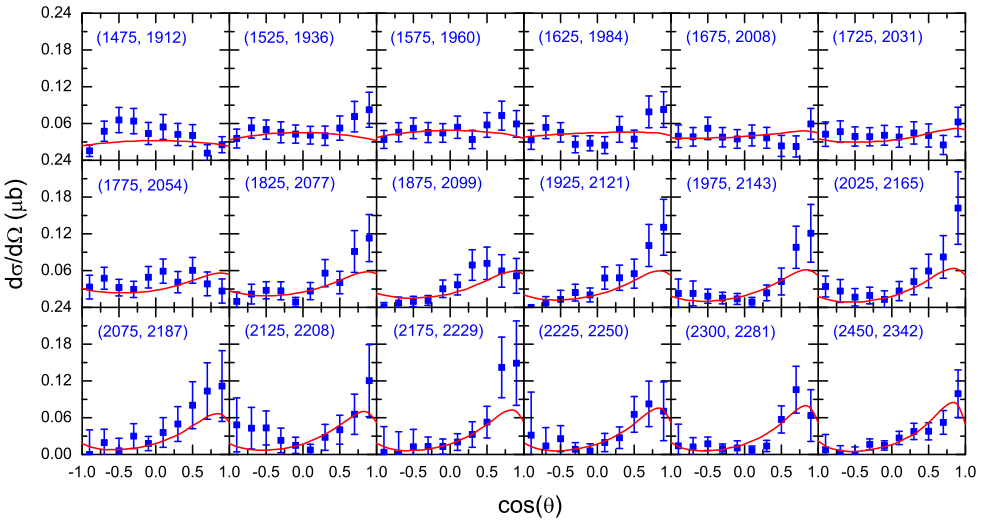

Fig. 3. (Color online) Differential cross sections for quasi-free $\gamma n \to \eta' n$. The solid curves are our results fitted to the CBELSA/TAPS quasi-free data [3] (solid squares).

3 Summary

We have performed a combined analysis [5] of the η' production reactions: $\gamma N \to \eta' N$, $NN \to NN\eta'$ and $\pi N \to \eta' N$. We found that a minimum set of three above-threshold resonances $\{S_{11}, P_{11}, P_{13}\}$, with the masses of about $M_R = 1925$, 2130 and 2050 MeV, respectively, and one below-threshold resonance $P_{13}(1720)$ is needed to describe all the existing data in the resonance-energy region up to $\sqrt{s} = 2.35$

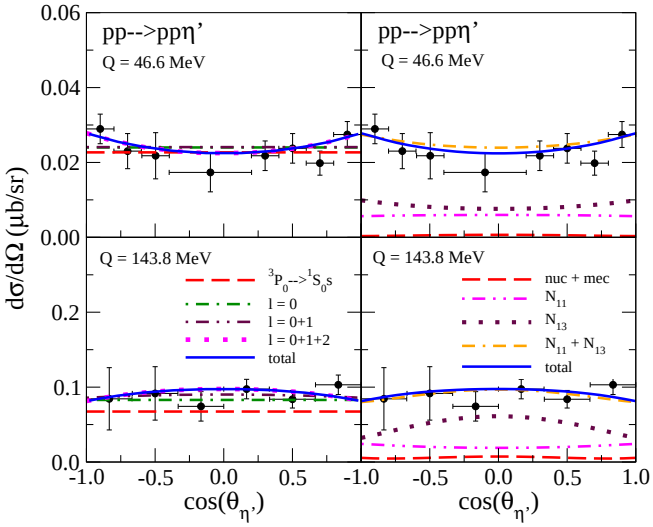

Fig. 4. (Color online) η' angular distribution in $pp \rightarrow pp\eta'$ in the center-of-momentum frame of the system for two excess energies of Q = 46.6 and 143.8 MeV. The solid curves show our results from full calculation. The panels in left hand-side column show the contributions from the partial waves, and the panels in the right-hand-side column show the contributions from individual currents. See Ref. [5] for more details.

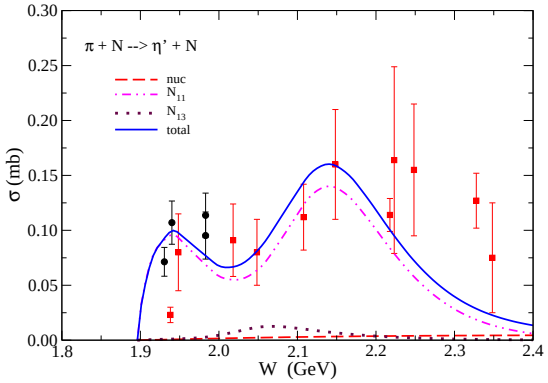

Fig. 5. (Color online) Total cross sections for $\pi N \rightarrow \eta' N$. The (blue) solid curves corresponds to the full results. See Ref. [5] for explanation of the contributions from individual currents.

GeV. These three above-threshold resonances may be tentatively identified with the corresponding $S_{11}(1895)$**, $P_{11}(2100)$*, and $P_{13}(2040)$* resonances listed in PDG [4].

References

1. M. Williams *et al.*, Phys. Rev. C **80**, 045213 (2009).
2. V. Crede *et al.*, Phys. Rev. C **80**, 055202 (2009).
3. I. Jaegle *et al.*, Eur. Phys. J. A **47**, 11 (2011).
4. J. Beringer *et al.* (Particle Data Group), Phys. Rev. D **86**, 010001 (2012).
5. F. Huang, H. Haberzettl, and K. Nakayama, arXiv:1208.2279.